Pergamon

Int. J. Heat Mass Transfer. Vol. 39, No. 8, pp. 1711–1718, 1996

0017-9310/96 $15.00+0.00

0017-9310(95)00218-9

Finite element simulations involving simultaneous multiple interface fronts in phase change problems

TIANHONG OUYANG and KUMAR K. TAMMA†

Department of Mechanical Engineering, Institute of Technology, 111 Church Street, S.E., University of Minnesota, Minneapolis, MN 55455, U.S.A.

(*Received* 16 *March* 1995 *and in final form* 1 *June* 1995)

Abstract—The present paper describes the simulation of phase change problems involving simultaneous multiple interface fronts employing the finite element method. Much of the past investigations employing finite elements have been restricted to primarily a single phase change situation. The existence of more than one phase, that is, the presence of multiple phase fronts poses certain challenges and further complications. However, the results provide a very interesting thermal behavior for this class of problems. In this paper, attention is focused on fixed grid methods and the trapezoidal family of one-step methods using the enthalpy formulations. Illustrative examples which handle simultaneous multiple fronts in phase change problems are presented.

INTRODUCTION

Numerous applications involving thermal heat conduction with phase change are of interest in advanced spacecraft and space station technology, and the problems related to various forming processes, ablation, castings, solar energy related applications, energy storage, etc. For certain materials the phenomenon of phase change occurs over a wide band of temperature ranges. Such problems permit fairly reasonable approximations to physically model the situation. For several other materials, the phase change phenomenon takes place instantaneously with almost no temperature variation. These problems are characterized by a Dirac-δ-type behavior and are slightly more difficult to handle computationaly. Over the years, a number of analytical and numerical approaches have been attempted for the above situations. To-date, one can reasonably expect to simulate these problems with certain amount of confidence. Both 'finite difference' and 'finite elements' have been extensively employed over the years. However, because of the several inherent advantages of the finite element method to handle complex geometries, treatment of boundary conditions, ability to interface with thermal-stress models for evaluating residual stresses, and the like, there is increased attention in employing the finite element method which is the chosen method in the present paper.

The predominant classes of techniques which can be identified in literature are the so called 'fixed grid' and 'front tracking' techniques with deforming grids. Whereas the former is fairly robust and most commonly employed due to its simplicity in coding effort and capability to handle general phase change situations with the phase front evaluated from the calculated temperature field, in the latter, the temperature field and the location of the phase fronts are both variables. Here, continuous monitoring of the phase front position is crucial and implementation aspects are rather cumbersome. The predominant classes of methods which can be identified in literature encompass the 'apparent heat capacity methods', the 'fictitious heat flow', or 'source based methods', and 'enthalpy based methods'. All of these have been quite extensively used and the pros and cons are well documented in literature [1–5] and references thereof. The predominant classes of solution schemes employing the finite element method which can be identified in literature for handling phase change problems include the generalized trapezoidal family of one-step methods [6], the Dupont II scheme [7], and the scheme due to Lees [8]. Both implicit and explicit solution strategies have been utilized for the simulation of phase change phenomenon. While explicit methods suffer from the drawbacks of conditional stability, they are relatively more easy to code than the corresponding implicit methods which have the advantage of unconditional stability. Although explicit methods require less computational effort per time step than the implicit counterparts, many analysts prefer the implicit formulations, which, for the total duration of the transient analysis are cited to be computationaly less expensive. In comparison to traditional practices for phase change problems, more recent research efforts due to Tamma and Namburu [5] and Namburu and Tamma [9] identify alternate

† Author to whom correspondence should be addressed.

NOMENCLATURE

c	specific heat
C_{AHC}	specified as $\partial H/\partial\theta$
c_s, c_L	specific heat of solid and liquid, respectively
c_m	specific heat in the freezing interval
$\mathbf{C}$	system capacitance matrix
h	convection coefficient
H	enthalpy function
k	thermal conductivity
k_{ij}	components of the element conductivity matrix
$\mathbf{K}$	system conductance matrix
$\mathscr{L}$	latent heat
N_α	element interpolation functions
Q	internal heat generation per unit volume
$\mathbf{Q}$	system heat load vector
R	domain
∂R	boundary
t	time level
ρ	density
ρ_s, ρ_L	density for solid and liquid, respectively
ρ_m	density in the freezing interval
$\boldsymbol{\theta}$	temperature vector
$\boldsymbol{\theta}_0$	initial temperature vector
θ_m	melting temperature
$\Delta\theta$	half temperature range over which phase change occurs
σ	Stefan-Boltzmann constant
ε	emissivity
α	stability parameter for time integration.

Subscripts

n	time level
s, L	solid and liquid phases, respectively
m	freezing interval representation.

formulations which employ flux-based representations and enthalpy formulations which possess several computationally attractive features, wherein, for certain phase change problems, explicit forms are competitive to implicit forms, although both are indeed applicable for handling general situations.

Many of the past investigations employing finite elements have been restricted to a single phase change situation. The existence of more than one phase, that is, the simultaneous presence of multiple phase fronts, poses certain challenges and further complications. It is in this regard that the present paper seeks to describe the transient thermal behavior employing the finite element method for accommodating the co-existence of simultaneous multiple phases. For illustrative purposes, attention is confined to fixed grid techniques although front tracking methods may also be applied. Williams and Curry [10] employ finite difference formulations and analyze a one-dimensional two phase multi-interface Stefan problem and provide interesting results. Motivated by technical discussions with Curry(author of ref. [10]) about multi-interface phase change problems in general, and its importance for several practical situations, the present paper describes the formulations, applicability and simulation of phase change problems with simultaneous multiple phases employing the finite element method. In particular, the simultaneous existence of two and three interface phase front situations is presented although one may generalize to the co-existence of any arbitrary number of phases and the associated thermal interactions and behavior. Numerical examples are presented which accommodate multiple phase fronts and therein describe the transient thermal behavior for a variety of situations.

MATHEMATICAL MODEL

The governing model equations following the classical theory of nonlinear heat conduction in domain R are given by:

$$\rho c_v(\theta)\frac{\partial\theta}{\partial t} = (k_{ij}\theta_{,j})_{,i} + Q \quad (x_i, t) \in R \times (0, T), \quad (1)$$

where ρ is the density, c_v is the specific heat, k_{ij} is the symmetric thermal conductivity tensor, Q is the generated internal heat flow source per unit volume and θ is the temperature field. Let R be enclosed by a boundary surface $\partial R = \partial R_p \cup \partial R_q$ where ∂R_p and ∂R_q are non-overlapping subregions of ∂R which consists of the prescribed temperature field boundary ∂R_p and the natural flux boundary ∂R_q.

The boundary and initial conditions are typically represented as

$$\theta = \theta_p \quad \text{on } \partial R_p \quad (2)$$

$$q_i n_i + q_s - h(\theta - \theta_h) - \sigma\varepsilon(\theta^4 - \theta_r^4) = 0 \quad \text{on } \partial R_q \quad (3)$$

and

$$\theta(x_i, t = 0) = \theta_i \quad x_i \in R. \quad (4)$$

Equations (1)–(4) refer to unsteady nonlinear thermal fields with thermophysical properties dependent upon temperature. The quantities θ_s, $\theta_h = h(\theta - \theta_h)$, and $\theta_r = \sigma\varepsilon(\theta^4 - \theta_r^4)$, represent surface heating per unit area, the rate of heat flux per unit area due to convection, and the heat flux rate per unit area due to radiation, respectively, on ∂R_q.

Focusing attention on fixed grid techniques for the numerical simulation of general multi-phase change

problems, the interface position is generally at some unknown location in the element. The evolution of the latent heat can be treated in terms of the thermophysical properties (specific heat) which are temperature dependent. Introducing the enthalpy function defined as

$$H = \int_{\theta_{\text{ref}}}^{\theta} \rho c(\theta)\, \mathrm{d}\theta, \tag{5}$$

where θ_{ref} is a reference temperature, for the classical Stefan problem one can write

$$H = \int_{\theta_{\text{ref}}}^{\theta} \rho c_{\text{s}}(\theta)\, \mathrm{d}\theta \quad (\theta < \theta_{\text{m}}) \tag{6a}$$

$$H = \int_{\theta_{\text{ref}}}^{\theta_{\text{m}}} \rho c_{\text{s}}(\theta)\, \mathrm{d}\theta + \rho \mathscr{L} + \int_{\theta_{\text{m}}}^{\theta} \rho c_{\text{L}}(\theta)\, \mathrm{d}\theta \quad (\theta > \theta_{\text{m}}), \tag{6b}$$

where the subscripts s and L denote the solid phase and liquid phase, respectively, $\mathscr{L}$ denotes the latent heat, and θ_{m} represents the melting temperature.

In the numerical implementation, this direct evaluation requires spreading the phase change across a temperature interval and thus introducing a phase change (melting or freezing) range. This phase change range must be kept small to avoid too much deviation from the original phase change (freezing or melting) problem (Stefan problem). To account for the finite phase change interval $[\theta_{\text{m1}}, \theta_{\text{m2}}]$, the enthalpy may be approximated as

$$H = \int_{\theta_{\text{ref}}}^{\theta} \rho_{\text{s}} c_{\text{s}}(\theta)\, \mathrm{d}\theta \quad (\theta < \theta_{\text{m1}}) \tag{7a}$$

$$H = \int_{\theta_{\text{ref}}}^{\theta_{\text{m1}}} \rho_{\text{s}} c_{\text{s}}(\theta)\, \mathrm{d}\theta + \int_{\theta_{\text{m1}}}^{\theta} \left[\rho_m \frac{\mathscr{L}}{2\Delta\theta} + \rho_m c_m(\theta) \right] \mathrm{d}\theta \quad (\theta_{\text{m1}} < \theta < \theta_{\text{m2}}) \tag{7b}$$

$$H = \int_{\theta_{\text{ref}}}^{\theta_{\text{m1}}} \rho_{\text{s}} c_{\text{s}}(\theta)\, \mathrm{d}\theta + \rho_m \mathscr{L} + \int_{\theta_{\text{m1}}}^{\theta_{\text{m2}}} \rho_m c_m(\theta)\, \mathrm{d}\theta + \int_{\theta_{\text{m2}}}^{\theta} \rho_{\text{L}} c_{\text{L}}(\theta)\, \mathrm{d}\theta \quad (\theta > \theta_{\text{m2}}), \tag{7c}$$

where $\theta_{\text{m1}} = \theta_{\text{m}} - \Delta\theta$ and $\theta_{\text{m2}} = \theta_{\text{m}} + \Delta\theta$ and $\Delta\theta$ is a half-temperature range over which phase change occurs. The quantities $c_m = \frac{1}{2}(c_{\text{s}} + c_{\text{L}})$ and $\rho_m = \frac{1}{2}(\rho_{\text{s}} + \rho_{\text{L}})$ are the specific heat and density in the freezing or melting interval.

Introducing the definition of enthalpy into the model equation (1), leads to

$$\frac{\partial H}{\partial t} = (k_{ij}\theta_{,j})_{,i} + Q \quad (x_i, t) \in R \times (0, T) \tag{8a}$$

or equivalently

$$\left(\frac{\partial H}{\partial \theta}\right)\left(\frac{\partial \theta}{\partial t}\right) = (k_{ij}\theta_{,j})_{,i} + Q \quad (x_i, t) \in R \times (0, T) \tag{8b}$$

or

$$C_{\text{AHC}}\dot{\theta} = (k_{ij}\theta_{,j})_{,i} + Q \quad (x_i, t) \in R \times (0, T), \tag{8c}$$

where $C_{\text{AHC}} = \partial H / \partial \theta$.

Finite element discretization

The finite element discretization is briefly described next and follows the standard classical Galerkin procedures. Introducing the approximation

$$\theta_{\text{e}} = N_\alpha \theta_\alpha, \tag{9}$$

where N_α are the element interpolation functions into equation (8c), a residual is obtained. Multiplying the residual by a weighting function ($W_\alpha = N_\alpha$) and integrating over the domain R, the resulting discretized representations are typically obtained as

$$\mathbf{C}(\boldsymbol{\theta})\dot{\boldsymbol{\theta}} + \mathbf{K}(\boldsymbol{\theta})\boldsymbol{\theta} = \mathbf{Q}(\boldsymbol{\theta}), \tag{10}$$

where

$$\mathbf{C} = \sum^{\text{e}} \int_{R_{\text{e}}} \mathbf{C}_{\text{AHC}} N_\alpha N_\beta \, \mathrm{d}R \tag{11}$$

$$\mathbf{K} = \sum^{\text{e}} \int_{R_{\text{e}}} k_{ij} N_{\alpha,i} N_{\beta,j} \, \mathrm{d}R + \sum^{\text{e}} \int_{\partial R_q} (h + \alpha_{\text{r}}) N_\alpha N_\beta \, \mathrm{d}R \tag{12}$$

$$\mathbf{Q} = \sum^{\text{e}} \int_{R_{\text{e}}} Q N_\alpha \, \mathrm{d}R + \sum^{\text{e}} \int_{R_q} N_\alpha (q_{\text{s}} + h\theta_{\text{h}} + \alpha_{\text{r}}\theta_{\text{r}}) \, \mathrm{d}R \tag{13}$$

and the summations are taken over the contributions of each element R_{e} in R. The term α_{r} is given by

$$\alpha_{\text{r}} = \sigma\varepsilon(\theta^2 + \theta_{\text{r}}^2)(\theta + \theta_{\text{r}}), \tag{14}$$

where θ_{r} is the radiation equilibrium temperature.

Time discretization

For the time discretization, the trapezoidal family of one-step α-methods is quite popular although other schemes as mentioned earlier have been used [1–5].

$$\mathbf{C}\dot{\boldsymbol{\theta}}_{n+1} + \mathbf{K}\boldsymbol{\theta}_{n+1} = \mathbf{Q}_{n+1} \tag{15a}$$

$$\boldsymbol{\theta}_{n+1} = \boldsymbol{\theta}_n + \Delta t \dot{\boldsymbol{\theta}}_{n+\alpha} \tag{15b}$$

$$\dot{\boldsymbol{\theta}}_{n+\alpha} = (1-\alpha)\dot{\boldsymbol{\theta}}_n + \alpha\dot{\boldsymbol{\theta}}_{n+1}, \tag{15c}$$

where Δt denotes the time step. α is a free parameter which controls the stability and accuracy of the scheme and is usually taken to be $0 \leqslant \alpha \leqslant 1$. Experience indicates that the $\alpha = 1$ (Euler-backward) with a lumped capacitance is the most favorable of the α-methods and is adopted here.

Considerations in phase change modeling/tracking the fronts

In the numerical simulation of phase change problems, approximating the term C_{AHC} in the capacitance matrix equation (11) is a critical step. Various approximation methods have been suggested and they are well documented in refs. [1–5]. In the present study, we restrict attention to that due to Del Guidice *et al.* [11] which has been cited to yield satisfactory results

$$C_{AHC} = \frac{\left[\left(\frac{\partial H}{\partial x}\right)\left(\frac{\partial \theta}{\partial x}\right)+\left(\frac{\partial H}{\partial y}\right)\left(\frac{\partial \theta}{\partial y}\right)+\left(\frac{\partial H}{\partial z}\right)\left(\frac{\partial \theta}{\partial z}\right)\right]}{\left[\left(\frac{\partial \theta}{\partial x}\right)^2+\left(\frac{\partial \theta}{\partial y}\right)^2+\left(\frac{\partial \theta}{\partial z}\right)^2\right]}, \tag{16}$$

where the enthalpy H rather than the heat capacity is also interpolated [12, 13] as follows:

$$H = N_\alpha H_\alpha, \tag{17}$$

where the N_α are the shape functions and H_α are the nodal values of the enthalpy.

When employing fixed grid methods for phase change problems involving a single face front, it is customary to first evaluate the temperature field and then evaluate the interface position by identifying elements whose nodal points are just above/below the melting/freezing temperature. In contrast to this, for the numerical simulation of phase change problems involving the existence of simultaneous multiple phase fronts, often, there are situations which arise at certain time points of the transient, wherein element temperatures over some of the regions in the domain closely approximate the actual melting/freezing temperature. This causes numerical difficulties in physically locating the interface positions. Regardless of the finite element space discretization, since adjacent element nodal values of temperature are in close proximity to the actual melting/freezing temperature, there may be a band of spatial locations which may likely seem to satisfy the criterion for locating the front position when they are interpolated upon. In view of these considerations, in the present study, the actual melting/freezing temperature is replaced as

$$\theta^*_{m,f} = \theta_{m,f} + \delta\theta, \tag{18}$$

where $\theta^*_{m,f}$ is the approximated melting/freezing temperature and $\delta\theta$ is a small incremental temperature field. Therein, the interface positions are interpolated upon in a straightforward manner employing the criterion

$$|\theta_i - \theta^*_{m,f}| < \varepsilon_{tol}, \tag{19}$$

where ε_{tol} is a user specified tolerance.

NUMERICAL EXAMPLES

This section presents the numerical simulation of phase change problems involving the simultaneous existence of multiple phase fronts employing the finite element method. The enthalpy model described previously is adopted here in conjunction with the Euler-backward ($\alpha = 1$) one-step solution scheme. The capacitance was assumed to be lumped and the approximation technique of Del Guidice *et al.* [11] is used.

The thermal models tested in the present study involved: (a) water, and/or (b) tin as the substances and the thermophysical properties and relevant data are taken from ref. [10] and are depicted in Table 1. The numerical models were evaluated for both substances in examples 1–3 and were evaluated for water substance in examples 4–6.

Example 1: *liquid–solid–liquid.*

$$\theta_{initial} = \theta_m + 55.56\text{K} \qquad t = 0$$
$$\theta_0 = \theta_m - 55.56\text{K} \quad 0 < t \leqslant 1000\text{s}$$
$$\theta_0 = \theta_m + 111.11\text{K} \qquad t > 1000\text{s}.$$

Example 2: *liquid–solid–liquid.*

$$\theta_{initial} = \theta_m + 55.56\text{K} \qquad t = 0$$
$$\theta_0 = \theta_m - 55.56\text{K} \quad 0 < t \leqslant 1000\text{s}$$
$$\theta_0 = \theta_m + 27.78\text{K} \qquad t > 1000\text{s}.$$

Example 3: *solid–liquid–solid.*

$$\theta_{initial} = \theta_m - 55.56\text{K} \qquad t = 0$$
$$\theta_0 = \theta_m + 55.56\text{K} \quad 0 < t \leqslant 1000\text{s}$$
$$\theta_0 = \theta_m - 27.78\text{K} \qquad t > 1000\text{s}.$$

Examples 1, 2, and 3 were analyzed until completion of all phase changes in each of the substances, namely water and tin, respectively. These examples involve the simultaneous presence of two interface phase fronts. There were 40 linear two-noded elements employed for the one dimensional models and a uniform time step $\Delta t = 5.0$ s was used.

Figures 1–6 depict the numerical simulations for each of the substances, namely, water and tin, respectively. The transient temperature variations and the locations of the multiple-phase fronts (freezing and melting phase fronts) are also presented for each test case.

Figure 1a presents the temperature history while Fig. 1b presents the phase fronts location for example 1 (water substance). It is interesting to note that in this example, during the initial stages ($t < 1000$) there is only one moving phase front (freezing front) and later on in the transient ($t > 1000$), the second phase front (melting front) is initiated at time $t > 1000$ s via the change of the associated boundary conditions. For the second stage, $t > 1000$, from the time of initiation of the melting front, the initial freezing phase front now no longer progresses ahead, but interestingly traverses backward while the second phase front moves forward until the two phase fronts coalesce after a certain time lapse, thereby, resulting in a single phase

Table 1. Thermal properties of water and tin

Thermal properties	Water	Tin
Heat conductivity of solid K_S	2.179 W $(m \cdot K)^{-1}$	58.8 W $(m \cdot K)^{-1}$
Heat conductivity of liquid K_L	0.588 W $(m \cdot K)^{-1}$	33.55 W $(m \cdot K)^{-1}$
Specific heat of solid c_S	1966.48 J $(kg \cdot K)^{-1}$	225.936 J $(kg \cdot K)^{-1}$
Specific heat of liquid c_L	4184.00 J $(kg \cdot K)^{-1}$	259.408 J $(kg \cdot K)^{-1}$
Density of solid ρ_S	921.1 kg m^{-3}	7304.4 kg m^{-3}
Density of liquid ρ_L	999.6 kg m^{-3}	6687.9 kg m^{-3}
Latent heat L	334720 J kg^{-1}	59040.9 J kg^{-1}
Melting temperature θ_m	273 K	505.22 K

(liquid phase). The locations and times of the various phases existing in the material has numerous practical benefits for engineering applications involving freezing and melting.

Figure 2 presents the thermal behavior, namely, temperature histories and multiple phase front position histories of example 2 in water substance. The phase front development process is similar to that of example 1 but the second stage involves a longer time period since the boundary conditions are different. Figure 3 shows the results for example 3 (water substance), which is solid–liquid–solid case in comparison to the previous examples which represent liquid–solid–liquid case. In this example, the time period for the initial front to traverse backward is significantly smaller. Figures 4–6 show the results for examples 1–3 with the substance being tin instead of water and a similar phenomenon can be seen for temperature and phase front histories. The results presented agree qualitative with those in ref. [10]. Unlike single phase change problems, the results presented provide a unique thermal behavior of the initial phase front progress and its interaction (attraction) with the second front. The results also clearly provide an understanding of the phase change phenomenon when simultaneous multiple phase fronts are involved.

The examples that follow next illustrate the situations when more than two phase fronts exist simultaneously for water substance only. In these examples, 40 linear two-noded elements and uniform time

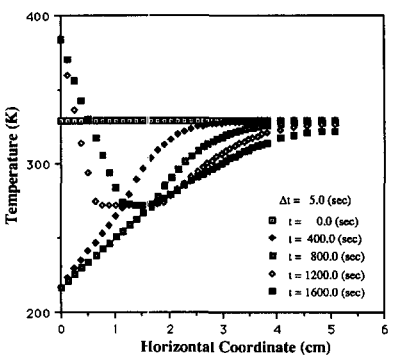

a). Temperature as function of space coordinate.

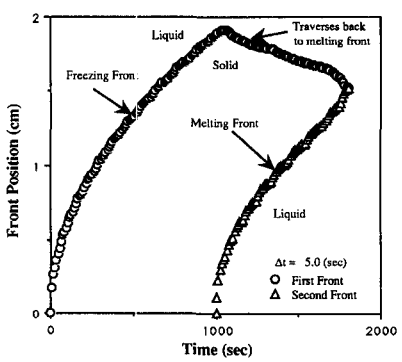

b). Front positions as a function of time.

Fig. 1. Temperature distributions and front positions (water, example 1). (a) Temperature as a function of space coordinate. (b) Front positions as a function of time.

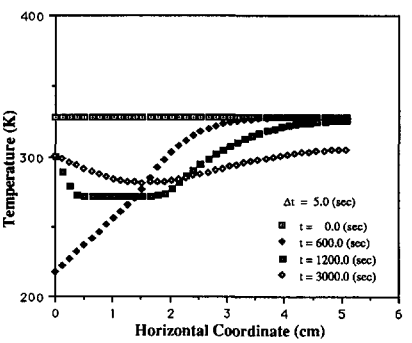

a). Temperature as function of space coordinate.

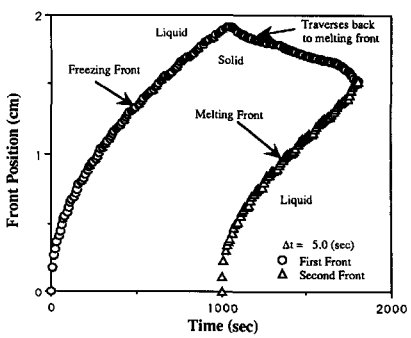

b). Front positions as a function of time.

Fig. 2. Temperature distributions and front positions (water, example 2). (a) Temperature as a function of space coordinate. (b) Front positions as a function of time.

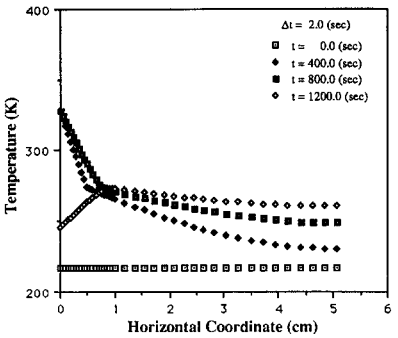

a). Temperature as function of space coordinate.

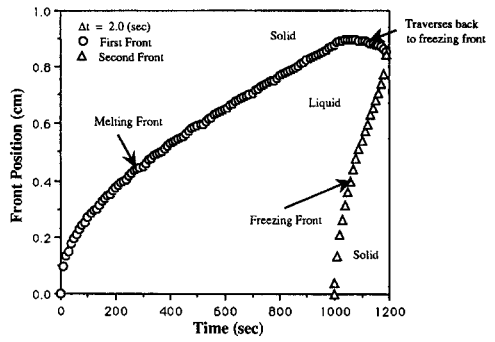

b). Front positions as a function of time.

Fig. 3. Temperature distributions and front positions (water, example 3). (a) Temperature as a function of space coordinate. (b) Front positions as a function of time.

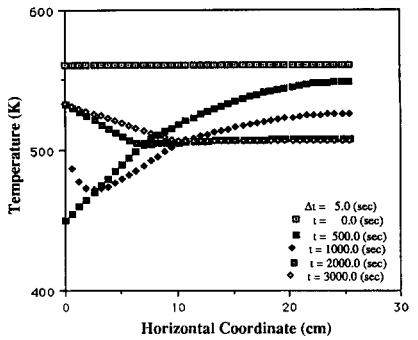

a). Temperature as function of space coordinate.

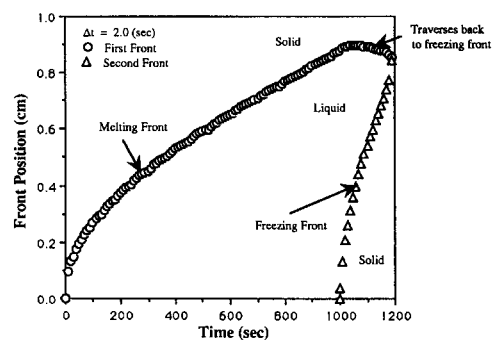

b). Front positions as a function of time.

Fig. 5. Temperature distributions and front positions (tin, example 2). (a) Temperature as a function of space coordinate. (b) Front positions as a function of time.

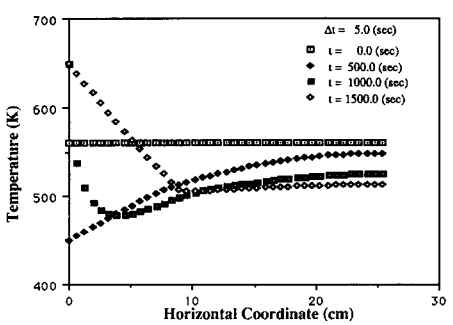

a). Temperature as function of space coordinate.

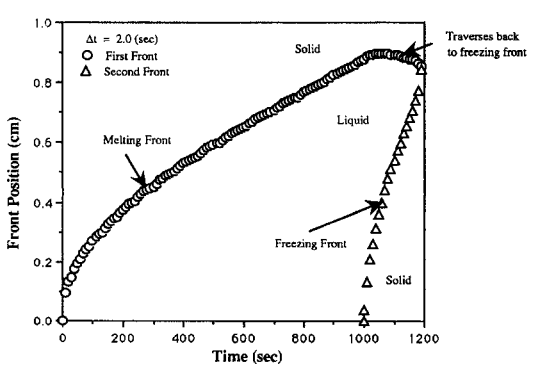

b). Front positions as a function of time.

Fig. 4. Temperature distributions and front positions (tin, example 1). (a) Temperature as a function of space coordinate. (b) Front positions as a function of time.

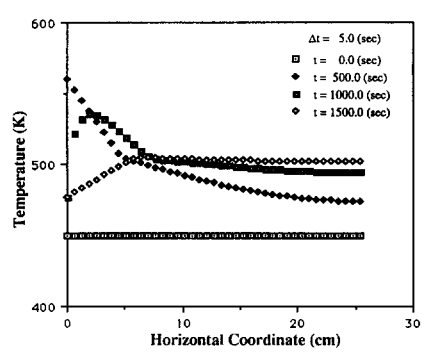

a). Temperature as function of space coordinate.

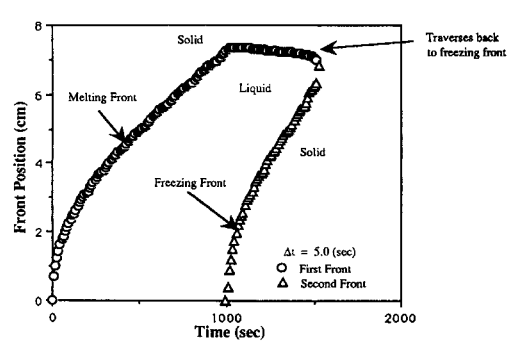

b). Front positions as a function of time.

Fig. 6. Temperature distributions and front positions (tin, example 3). (a) Temperature as a function of space coordinate. (b) Front positions as a function of time.

step $\Delta t = 5.0$ s were employed which involve the simultaneous existence of the three interface fronts. The thermal behavior for these situations also has numerous practical benefits and the physical process of phase change is of fundamental importance here.

Example 4: *liquid–solid–liquid–solid.*

$$\begin{aligned}
\theta_{\text{initial}} &= \theta_m + 55.56\text{K} && t = 0\\
\theta_0 &= \theta_m - 55.56\text{K} && 0 < t \leqslant 1000\text{ s}\\
\theta_0 &= \theta_m + 111.11\text{K} && 1000 < t \leqslant 1500\text{ s}\\
\theta_0 &= \theta_m - 55.56\text{K} && t > 1500\text{ s}.
\end{aligned}$$

Example 5: *liquid–solid–liquid–solid.*

$$\begin{aligned}
\theta_{\text{initial}} &= \theta_m + 55.56\text{K} && t = 0\\
\theta_0 &= \theta_m - 55.56\text{K} && 0 < t \leqslant 1000\text{s}\\
\theta_0 &= \theta_m + 27.78\text{K} && 1000 < t \leqslant 2000\text{s}\\
\theta_0 &= \theta_m - 55.56\text{K} && t > 2000\text{s}.
\end{aligned}$$

Example 6: *solid–liquid–solid–liquid.*

$$\begin{aligned}
\theta_{\text{initial}} &= \theta_m - 55.56\text{K} && t = 0\\
\theta_0 &= \theta_m + 55.56\text{K} && 0 < t \leqslant 1000\text{s}\\
\theta_0 &= \theta_m - 27.78\text{K} && 1000 < t \leqslant 1120\text{s}\\
\theta_0 &= \theta_m + 55.56\text{K} && t > 1120\text{s}.
\end{aligned}$$

Figures 7–9 depict the numerical simulations for water substance for examples 4–6, respectively, in one-dimensional models. The phase front locations with time for each case are presented here. From Fig. 7, one can see that in example 4, during the initial stages ($t < 1000$) there is only one progressing phase front (freezing front) and later on in the second stage ($1000 \leqslant t \leqslant 1500$), the second phase front (melting front) is initiated at which time the initial progressing front now traverses backward and changes into a melting front from a freezing front. During the third stage, $t \leqslant 1500$ in example 4, a third front (freezing front) is initiated. At this point, there exist three phase fronts simultaneously. During the period $1500 \leqslant t \leqslant 1720$ s, the first front (now a melting front) continues to traverse back as a melting front while the second melting front continues to progress ahead to meet the third front until the liquid region between them shrinks and completely disappears. Note that the second front only takes a very short time period to traverse backward and change into a freezing front before it meets the third front. After a further time lapse, at about $t = 1820$ s, the first front changes back into a freezing front from a melting front and progresses forward. It is interesting to note that the third front and first front seem to appear as if a single front was discontinued during time period $1720 < t < 1820$, although they are entirely different fronts. This phenomenon is also evident in examples 5 and 6 (see Figs. 8 and 9) where example 6 is for the solid–liquid–solid–liquid case, while examples 4 and 5 are for the liquid–solid–liquid–solid case. It is noteworthy to see the development and interactions of the second and third phase fronts within a very short period of time in example 6. The last three examples clearly provide a better understanding of the multiple phase change phenomenon in periodic heating and cooling situations.

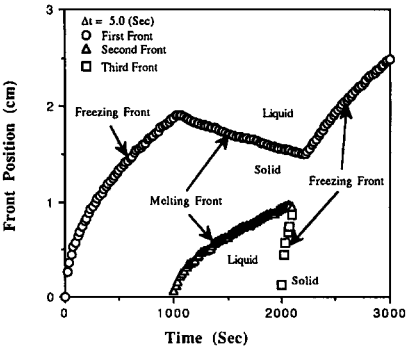

Fig. 8. Front positions as a function of time (water, example 5).

CONCLUDING REMARKS

The paper described the numerical simulation of phase change problems involving simultaneous multiple phase fronts via the finite element method. The enthalpy model simulations were employed in con-

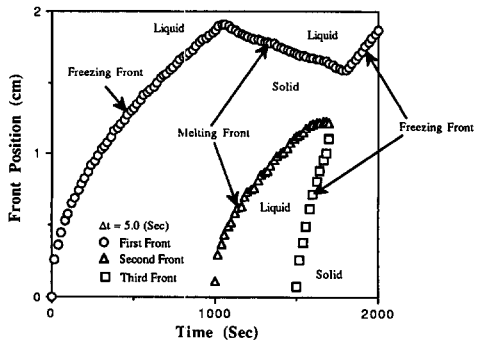

Fig. 7. Front positions as a function of time (water, example 4).

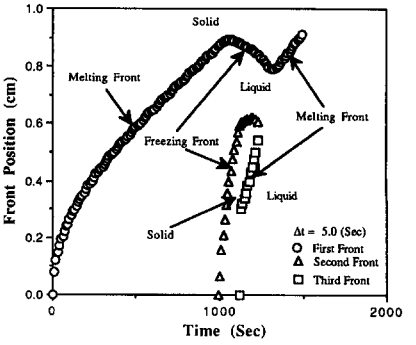

Fig. 9. Front positions as a function of time (water, example 6).

junction with the Euler-backward solution scheme and a lumped capacitance. Attention was restricted to simple two-noded linear elements. Numerical formulations were described with applications to two different substances, namely, water and tin, respectively, wherein, multiple phase fronts were simultaneously involved. The multi-interface problems provide a very interesting thermal behavior in contrast to single phase change problems and pose certain additional complexities. The results clearly describe the physics and nature of the thermal behavior and phase front interactions when simultaneous multiple phase fronts are involved.

Acknowledgements—The authors would like to acknowledge Dr D. M. Curry, NASA-Johnson Space Center, Houston, Texas for his encouragement and guidance. Excerpts of this research was supported, in part, by NASA-Langley Research Center in Hampton, Virginia under grant NAG-1-808 and the Flight Dynamics Laboratory, Wright Patterson Air Force, Ohio. The authors are also very pleased to acknowledge support, in part, by the Army High Performance Computing Research Center (AHPCRC) at the University of Minnesota, and the Minnesota Supercomputer Institute, Minneapolis, Minnesota. More recent support, in part, by Mr William Mermagen Sr, and Dr Andrew Mark of the ASMPCD at the Army Research Laboratory, APG, MD, is also greatly acknowledged.

REFERENCES

1. A. J. Dalhuijsen and A. Segal, Comparison of finite element techniques for solidification problems, *Int. J. Numer. Meth. Engng* **23,** 1807–1829 (1986).
2. B. G. Thomas, I. V. Samarasekara and K. Brimacombe, Comparison of numerical modeling techniques for complex two-dimensional transient heat conduction problems, *Met. Trans. B.* **15,** 307–318 (1984).
3. W. D. Rolph III and K. J. Bathe, An efficient algorithm for analysis of non-linear heat transfer with phase change, *Int. J. Numer. Meth. Engng* **18,** 119–134 (1982).
4. R. M. Furzeland, A comparative study of numerical methods for moving boundary problems, *J. Inst. Maths Appl.* **26,** 411–429 (1980).
5. K. K. Tamma and R. R. Namburu, Recent advances, trends and new perspective via enthalpy-based finite element formulations for applications to solidification problems, *Int. J. Numer. Meth. Engng* **30,** 803–820 (1990).
6. T. J. R. Hughes and T. Belytschko, A precis of developments in computational methods for transient analysis, *J. Appl. Mech. ASME* **50,** 1032–1041 (1983).
7. T. Dupont, G. Fairweather and J. P. Johnson, Three-level Galerkin methods for parabolic equations, *SIAM J. Numer. Anal.* **11,** 392–410 (1974).
8. M. Lees, A linear three-level difference scheme for quasi-linear parabolic problems, *Math. Comput.* **20,** 516–522 (1966).
9. R. R. Namburu and K. K. Tamma, Effective modeling/analysis of isothermal phase change problems with emphasis on representative enthalpy architectures and finite elements, *Int. J. Heat Mass Transfer* **36,** 4493–4497 (1993).
10. S. D. Williams and D. M. Curry, An implicit formulation for the one-dimensional two-phase multi-interface Stefan problems, ASME paper 82-HT-21 (1982).
11. S. Del Guidice, G. Comini and R. W. Lewis, Finite element simulation of freezing processes in soils, *Int. J. Numer. Anal. Meth. Geomech.* **2,** 223–235 (1978).
12. G. Comini, S. Del Guidice, R. W. Lewis and O. C. Zienkiewicz, Finite element solution of non-linear heat conduction problems with special reference to phase change, *Int. J. Numer. Meth. Engng* **8,** 613–624 (1974).
13. K. Morgan, R. W. Lewis and O. C. Zienkiewicz, An improved algorithm for heat conduction problems with phase change, *Int. J. Numer. Meth. Engng* **12,** 1191–1195 (1978).